Polymer Journal, Vol. 16, No. 2, pp 119—128 (1984)

Characterization of the Microstructure of Poly(propylene oxide)–Segmented Polyamide and Its Suppression of Platelet Adhesion

Nobuhiko YUI, Junko TANAKA, Kohei SANUI,
Naoya OGATA, Kazunori KATAOKA,*
Teruo OKANO,** and Yasuhisa SAKURAI**

Department of Chemistry, Faculty of Science and Technology, Sophia University, 7–1 Kioi-cho, Chiyoda-ku, Tokyo 102, Japan
**Heart Institute of Japan, Tokyo Women's Medical College, 10 Kawada-cho, Ichigaya, Shinjuku-ku, Tokyo 162, Japan*
***Institute of Medical Engineering, Tokyo Women's Medical College, 10 Kawada-cho, Ichigaya, Shinjuku-ku, Tokyo 162, Japan*

(Received September 12, 1983)

ABSTRACT: The relationship between microphase-separated structures and antithrombogenicities of poly(propylene oxide) (PPO)–segmented polyamides of various polyamide segment lengths was studied. Transmission electron microscopic observation revealed fibrillar lamella structures to be present on the copolymer surfaces. Dynamic mechanical and thermal scanning measurements showed the existence of two mechanical relaxations attributable to micro-Brownian motions of the PPO and polyamide segments, indicating that the PPO and polyamide segments formed distinctly separated microdomain structures. Moreover, wide-angle X-ray diffraction and small-angle X-ray scattering measurements indicated these copolymers to be different in their microstructures with respect to size and distribution of crystalline and amorphous domains even though the crystalline structure was essentially the same as that of nylon 610. The degree of platelet adhesion and aggregation was significantly minimized on the surface of the copolymer, in which the average diameter of the crystalline and amorphous domains were 6.42 nm and 5.18 nm, respectively. This suggests that the size of segmented polyamide microdomains may be a determining factor in antithrombogenicity.

KEY WORDS Microphase-Separated Structure / Poly(propylene oxide) / Nylon 610 / Crystallinity / Long Period / Platelet Adhesion / Microsphere Column Method / Polyamide /

Recently many polymeric materials have found clinical application in artificial organs, surgical implants, and many other prosthetic devices. Since polymeric materials generally show rejection such as thrombus formation and inflammation when in contact with biological systems, polymers for biomedical materials must have good biocompatibility.

It is known that the surface of a synthetic polymer forming a microphase-separated structure similar to heterogeneous surfaces of endothelium cells,[1] shows good antithrombogenicity.[2-7] Especially, a segmented copolyether–urethane–urea, known as Biomer,® has been widely used for cardiovascular prostheses such as blood pumps mainly because of its antithrombogenicity and excellent mechanical properties.[8-15] These favorable properties are considered due to the formation of a microphase-separated structure; clusters of hard segments are dispersed in a continuous phase of soft segments to form the domains. In regard to the domain structure, Lyman *et al.* assumed these copolymers to have two phase

morphology with domains of 3—10 nm.[11] Recently, Takahara *et al.* estimated that the size of hard and soft segment domains in these copolymers was 9.2 nm and 0.9—2.1 nm, respectively, from small-angle X-ray scattering measurements.[13,15] More detailed studies on various aspects of the morphology of these copolymers are now being carried out,[16-19] since the relationship between the microstructures of these copolymers and their blood compatibility is still not fully understood.

To clarify this relationship, Okano *et al.* developed hydroxyethyl methacrylate–styrene block copolymers having microphase-separated structures consisting of hydrophilic and hydrophobic microdomains.[3] The results of their study on the blood compatibility and adsorption behavior of plasma proteins with these copolymers indicate that a copolymer surface having an alternating lamellae structure 30—50 nm in width may be capable of suppressing platelet adhesion.[6,7] Thus, the "microdomain" structure performed an important role in antithrombogenicity of biomaterials.

In our systematic studies on the adhesion behavior of blood cells on condensation polymers, the higher-ordered structure of a polyamide, including distribution of crystalline regions and chemical structure have been found to play important roles in the adhesion of blood cells, platelets and leukocytes.[20-23] Thus control of the crystallinity of polyamide surfaces is a means for realizing ideal antithrombogenic surfaces.

In a previous paper,[24] it was reported that poly(propylene oxide) (PPO)–segmented polyamides synthesized by an interfacial polycondensation method exhibited a distinct phase separation of the PPO and polyamide segments. This paper reports the effects of copolymer microstructures on the interaction between the surfaces of copolymers and blood platelets. This interaction was studied by a microsphere column method.[25] The present results indicate that the size of microdomains of segmented polyamides may possibly be the most determinative factor involved in antithrombogenicity.

EXPERIMENTAL

Materials

PPO-segmented polyamides were prepared by interfacial polycondensation with vigorous stirring as reported previously.[24] The details are discussed only briefly here. PPO having carbonyl chloride groups at both ends with a molecular weight of 3000 was prepared by reacting PPO with an excess amount of sebacoyl chloride at 80—90°C for 6 h. The reaction mixture was dissolved in chloroform,

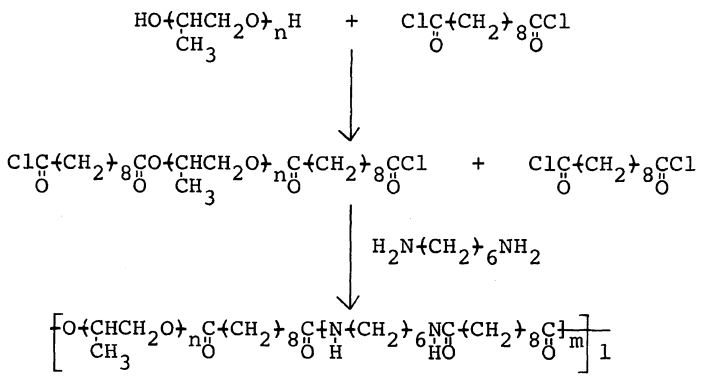

Figure 1. Synthesis of PPO–segmented polyamide.

Table I. Synthesis of PPO–segmented polyamides

Polymer		Elemental analysis/wt%			Weight fraction of PPO[a]	Molecular weight		η_{sp}/c[c]
		C	H	N		PPO segment	Polyamide segment[b]	
P-10	Found	68.6	9.9	9.2	0.083	3000	33200	1.68
	Calcd	68.8	9.9	9.1				
P-25	Found	61.5	9.7	6.8	0.25	3000	9200	2.05
	Calcd	68.0	9.1	8.0				
P-47	Found	64.8	10.2	5.0	0.47	3000	3400	1.55
	Calcd	65.2	9.7	4.2				

[a] Weight fraction of PPO in the copolymer was determined by elemental analysis.
[b] Molecular weight of the polyamide segment was determined by elemental analysis.
[c] 0.1 g/10 cm^3 in *m*-cresol at 30°C.

and then allowed to react with an aqueous solution of 1,6-hexanediamine in a blender to obtain the PPO–segmented polyamide as shown in Figure 1. Characterization of the copolymers is presented in Table I.

Transmission Electron Microscopic Observation

A 0.1 wt% *m*-cresol solution of a copolymer was cast on collodion- and carbon-coated nickel meshes and the thin films were prepared by evaporation at 60°C. After drying *in vacuo*, the film surface microstructure was observed by a transmission electron microscope (Hitachi HS-9) without the aid of staining.

Dynamic Mechanical Measurements

Measurements were made on a Vibron Dynamic Viscoelastometer (Toyo Baldwin DDV-II-EA). The temperature range was from −100°C to 200°C under a dry nitrogen atmosphere and the frequency employed was 11 Hz. The sample films used were made by solution casting of a 5 wt% *m*-cresol solution on glass plates and then dried *in vacuo* at 60°C.

Thermal Analysis

Thermal properties were measured by differential scanning calorimetry (DSC) with DSC calorimeters (Rigakudenki 8058D1 and 8055C1) at a heating rate of 20°C min^{-1}. The sample films were prepared by the procedure described above.

X-Ray Diffraction

Wide-angle X-ray diffraction (WAXD) and small-angle X-ray scattering (SAXS) measurements were recorded photographically using a Rotaflex (Rigakudenki RU-200) with nickel-filtered Cu$K\alpha$ radiation operated at 50 kV and 200 mA.

Estimation of Platelet Adhesion

One gram of polymer-precoated glass beads was packed in a tube of poly(vinyl chloride) and was subjected to the following platelet adhesion test: fresh blood, 3 cm^3, was collected from a jugular vein of a mongrel dog with a disposable syringe without anticoagulant and was immediately passed through the column packed with the glass beads in 60 s at a flow rate of 1.2 cm^3 min^{-1} using a Presidol model 5003 infusion pump. The eluted blood was collected along with the primed saline in a sample bottle containing 0.1 cm^3 of a sodium citrate solution as an anticoagulant. The column was then washed with a saline solution at a flow rate of 1.2 cm^3 min^{-1} for a period of 120 s. The beads in the upper part of the rinsed column were placed in a saline solution containing 1.25 wt% glutaraldehyde to fix the adhered platelets. The beads were then freeze-

dried and coated with gold. The surfaces of the beads were observed by a scanning electron microscope (SEM) (Hitachi S-430). More than 10 views per each sample were made and typical micrographs of various samples were taken. The number of platelets in the eluted blood was counted according to the method of Brecher and Cronkite.[26]

RESULTS AND DISCUSSION

Microstructures of PPO-Segmented Polyamides Films

A transmission electron micrograph of the

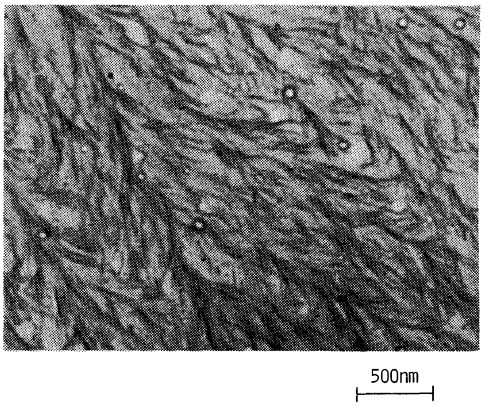

Figure 2. TEM view of PPO–segmented polyamide (P-25).

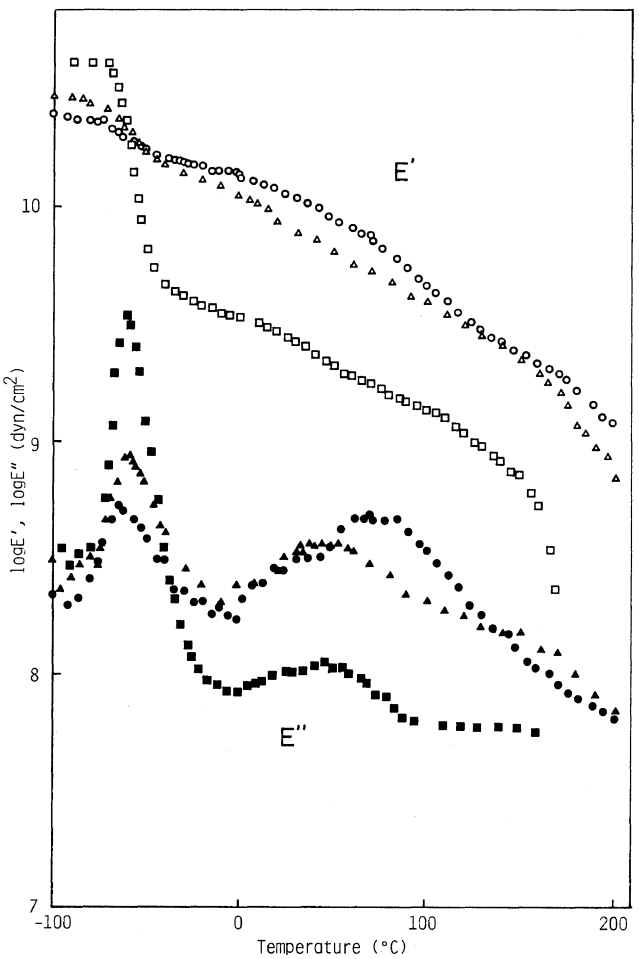

Figure 3. Temperature dependence of E' and E'' for PPO–segmented polyamides at 11 Hz. (○), P-10; (△), P-25; (□), P-47.

P-25 copolymer surface is shown in Figure 2. The light and dark regions of the micrograph correspond to the amorphous and crystalline regions of the copolymer, respectively. The micrograph indicates a microstructure consisting a fibrillar lamellae approximately 10—50 nm in thickness. This observation revealed that the microphase-separated structures of the copolymer surfaces may possibly consist of crystalline and amorphous regions.

Figure 3 shows the temperature dependence of the storage modulus (E') and loss modulus (E'') of the copolymers. In this figure, two mechanical relaxation regions corresponding to a decrease in E' and the E'' curve peaks can clearly be seen for each sample. The lower relaxation temperature (T_1) appeared at approximately -60°C, and the higher (T_2) at 40°C to 60°C. The magnitude of the E' decrease and peak height of E'' increased with increasing PPO weight fractions. These findings are characteristic of a microphase-separated structure of a copolymer formed by joining blocks of two chemically dissimilar segments, and thus it is likely that the PPO and polyamide segments form a microphase-separated structure in the copolymer.

Thermal scanning measurements showed two endotherms for each sample, one at about -60°C, owing to the glass transition temperature (T_g) of the PPO segment, and the second, at 220°C, corresponding to the melting temperature (T_m) of the polyamide segment. With T_g of PPO being -62.5°C, the T_1 relaxation may be attributed to micro-Brownian motions of PPO segments associated with their glass transition.[27] No endotherm corresponding to the glass transition of the polyamide segment in the copolymers was observed. A possible reason for this may be that, when the polyamide segment began micro-Brownian motions with increasing temperature, the transition occurred continuously rather than only throughout a narrow temperature range, as a result of the crystallinity of the polyamide segment. Because of the broadness of this T_g range, the DSC curves for the copolymers showed no endotherms corresponding to the T_g of the polyamide segment. A slight endotherm was observed at 55.8°C, thus indicating that the T_2 relaxation may possibly have arisen from the glass transition of the polyamide segment.[28] The broadness of the glass transition of the polyamide segment could be confirmed by the broad peak of E''.

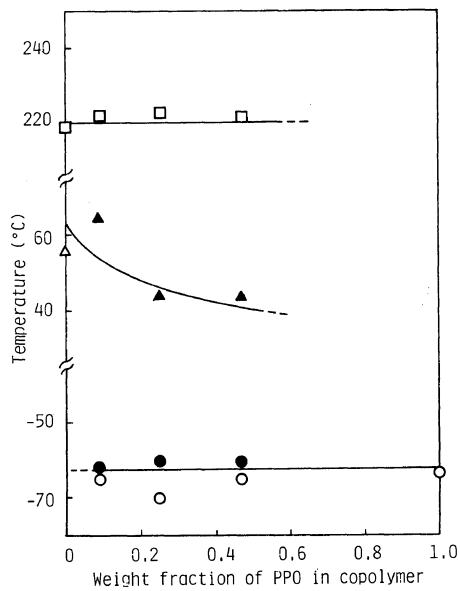

Figure 4. T_g and T_m of PPO–segmented polyamides. (○, ●), T_g for the PPO segment; (△, ▲), T_g for the polyamide segment; (□), T_m for the polyamide segment. Open plots were obtained from thermal analysis data and those closed from dynamic mechanical measurements.

T_g and T_m for the copolymers determined from the peak positions on the E'' curves and the endotherms on the DSC curves are shown in Figure 4, as functions of the weight fraction of the PPO segment in the copolymer. Generally, the rigidity of the polyamide segment domain was apparently controlled by the soft PPO segment domain, when a strong interfacial mixing between the PPO segment and polyamide domain was predominant. Actually, T_g of these segments and T_m of the polyamide segment were hardly influenced at

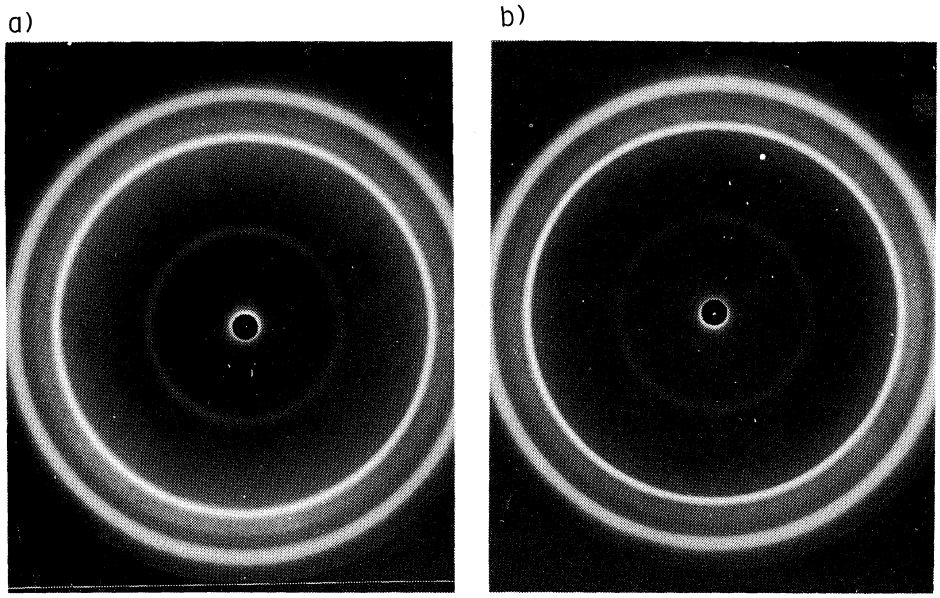

Figure 5. WAXD patterns of a), P-25; b), nylon 610.

Table II. Spacing of PPO–segmented polyamides as determined by WAXD measurements

Polymer	Bragg spacing/nm			
	d	*d'*	*d''*	*d'''*
Nylon 610	0.37	0.40	0.45	0.86
P-10	0.37	0.40	0.44	0.83
P-25	0.37	0.40	0.44	0.85
P-47	0.37	0.41	0.45	0.86

all by the existence of the PPO segments in the copolymer, indicating the presence of a distinct phase separation between the PPO and polyamide segments.

Figure 5 shows the WAXD patterns of a copolymer in which the PPO weight fraction was 0.25 and the homopolymer, nylon 610. The diffraction pattern of the copolymer was identical with that of nylon 610. Bragg's spacings determined from WAXD patterns are shown in Table II. From these results, it is evident that these copolymers had essentially the same basic structure as nylon 610 with respect to the crystal lattice or crystal structure.

The SAXS results can quantitatively be interpreted in terms of structural sub-units several dozen nanometers in size. The long period obtained from the SAXS patterns thus provides information on the effective density differences between the two phases, *i.e.*, a repeat distance composed of PPO and polyamide domains, as shown in Figure 6. Table III is a list of the copolymer long periods along with the lamella widths of the polyamide domains, and the average diameter of the amorphous phase between the lamellae regions. The lamella widths of the polyamide domains were calculated from the equation, $L' = L\phi\chi_c$, where L is a long period, ϕ, the volume fraction of the polyamide segments, and χ_c ($=0.758$), the degree of crystallinity of nylon 610 estimated by the density method. In this equation, it is assumed that the degree of crystallinity of polyamide domains in the copolymer is independent of the PPO content because of the presence of a distinct phase separation between the PPO and polyamide segments in the copolymer. With an increase in the weight

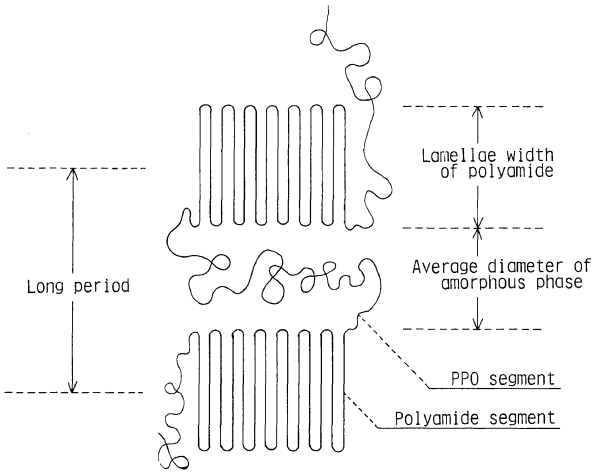

Figure 6. Schematic representation of the microphase-separated structure of PPO–segmented polyamide.

Table III. PPO–segmented polyamide microstructures

Polymer	Long period[a] / nm	Lamella width of[b] polyamide / nm	Average diameter of[c] amorphous phase / nm
Nylon 610	9.90	7.50	2.40
P-10	10.6	7.31	3.29
P-25	11.6	6.42	5.18
P-47	14.6	5.53	9.07

[a] Determined from SAXS measurements.
[b] $L' = L\phi\chi_c$ (L, long period; ϕ, volume fraction of nylon 610; χ_c, degree of crystallinity of nylon 610).
[c] $= L - L'$.

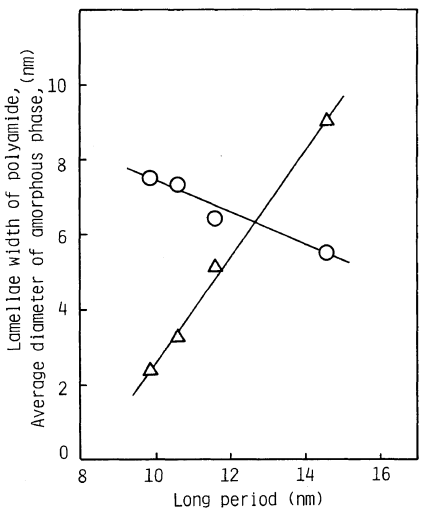

Figure 7. PPO–segmented polyamide microstructures. (○), lamella width of polyamide domains; (△), average diameter of amorphous phases between lamella regions.

fraction of the PPO segment in the copolymer, the long period increased, the lamella width of the polyamide domain decreased slightly, and the average diameter of the amorphous phase between the lamella regions increased, as shown in Figure 7. These results indicate that a series of the copolymers had different microstructures with respect to size and distribution of the crystalline and amorphous domains, but whose structures were basically the same structures as that described above. Thus, a series of the copolymers may possibly be suitable for model polymers in studying the effects of crystalline and amorphous domain microstructures on the adhesion of blood platelets.

Platelet Adhesion on PPO–Segmented Polyamides

Platelet adhesion and aggregation on for-

eign surfaces are the first observable steps in blood clotting. These phenomena are considered to play major roles in the *in vivo* initiation of thrombus formation on such surfaces.[29] Adhesion behavior on copolymer surfaces was examined in six dogs and the results were compared with those obtained for the homopolymer, nylon 610. The extent of platelet adhesion on each of various copolymer surfaces is summarized in Table IV. The copolymers exhibited suppressive effects on platelet adhesion and the number of adhered platelets decreased for the copolymer containing the 0.25 wt fraction of PPO. Blood platelet adhesion on copolymer surfaces was also examined by a scanning electron microscope. Figure 8 shows SEM views of adhered platelets on the surfaces of nylon 610, P-10, and P-25. For the surface of nylon 610, it was found that the adhered platelets aggregated by means of pseudopods. With copolymers, a few adhered platelets were observed on all copolymer surfaces and were discoid in shape, as shown in Figure 8, as was the case for the native form. These results show that the copolymers suppressed morphological change in adhered platelets and copolymer containing the 0.25 wt fraction of PPO showed a minimum amount of platelet adhesion.

Table IV. Platelet adhesion on PPO–segmented polyamide surfaces

Polymer	Amount of adhered platelets/%[a]
Nylon 610	27.2± 9.6
P-10	24.3± 7.8
P-25	14.1± 2.4
P-47	33.9±11

[a] The mean±S.E.M. 100%=whole blood.

A microphase-separated structure consisting of crystalline polyamide and amorphous PPO segments is the probable cause for this suppression. Figure 9 shows the relationship between platelet adhesion and magnitude of the polymer long period, which reflects the morphological characteristics of the polymer surface. In this figure, minimum platelet adhesion was noted for a copolymer having a long period of 11.6 nm, that is, the average diameter of the crystalline and amorphous domains of 6.42 and 5.18 nm, respectively. This suggests that the particular size and distribution of the crystalline and amorphous domains in a copolymer bears an important relation to platelet adhesion. Control of the phase separation of polyamide segments in these copolymers by regulation of copolymer composition, block length, and polyamide segment crystalliza-

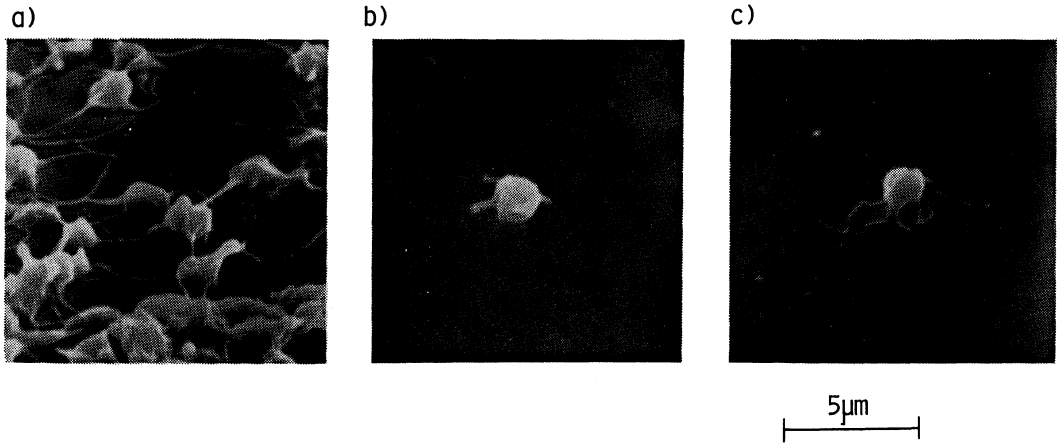

Figure 8. SEM views of platelets adhering to PPO–segmented polyamide surfaces, a), nylon 610; b), P-10; c), P-25.

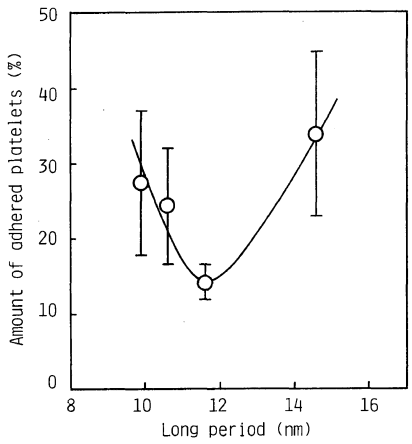

Figure 9. Relationship between platelet adhesion and PPO–segmented polyamide microstructures (±S.E.M.)

bility is thus an important factor in antithrombogenicity.

Acknowledgements. The authors are grateful to Prof. Motowo Takayanagi, Prof. Tisato Kajiyama, and Dr. Atsushi Kumano, Department of Applied Chemistry, Faculty of Engineering, Kyushu University, for their advice and assistance in making the WAXD and SAXS measurements, and to Mr. Atsushi Kasai, Mitsubishi Chemical Industry Co., for expediting the dynamic mechanical measurements. Thanks are also due to Mr. Masafumi Sano, Sophia University, for carrying out some of the experiments. This study was supported by the Ministry of Education, Japan (Special Project Research, "Design of Multiphase Biomedical Materials") and by the Japan Research Promotion Society for Cardiovascular Diseases.

REFERENCES

1. S. J. Singer and G. L. Nicolson, *Science*, **175**, 720 (1972).
2. Y. Imai, A. Watanabe, and E. Masuhara, *Jpn. J. Artif. Organs*, **2**, 95 (1973).
3. T. Okano, M. Katayama, and I. Shinohara, *J. Appl. Polym. Sci.*, **22**, 369 (1978).
4. K. Kataoka, T. Okano, T. Akaike, Y. Sakurai, M. Maeda, T. Nishimura, Y. Nitadori, T. Tsuruta, M. Shimada, and I. Shinohara, *Jpn. J. Artif. Organs*, **8**, 804 (1979).
5. Y. Sakurai, T. Akaike, K. Kataoka, and T. Okano, "Biomedical Polymers," E. P. Goldberg and A. Nakajima, Ed., Academic Press, New York, 1980, p 335.
6. T. Okano, S. Nishiyama, I. Shinohara, T. Akaike, Y. Sakurai, K. Kataoka, and T. Tsuruta, *J. Biomed. Mater. Res.*, **15**, 393 (1981).
7. T. Okano, M. Shimada, I. Shinohara, K. Kataoka, T. Akaike, and Y. Sakurai, "Advances in Biomaterials," Vol. 3, G. D. Winter, D. F. Gibbons, and H. Plenk, Ed., John Wiley, New York, 1982, p 445.
8. D. J. Lyman, C. Kwann-Gett, H. H. J. Zwart, A. Bland, N. Eastwood, J. Kawai, and W. J. Kolff, *Trans. ASAIO*, **17**, 456 (1971).
9. D. J. Lyman, D. W. Hill, R. K. Stirk, C. Adamson, and B. R. Mooney, *Trans. ASAIO*, **18**, 19 (1972).
10. D. J. Lyman, L. C. Metcalf, D. Albo, Jr., K. F. Richards, and J. Lamb, *Trans. ASAIO*, **20**, 474 (1974).
11. D. J. Lyman, K. Knotson, B. McNeil, and K. Shibatani, *Trans. ASAIO*, **21**, 49 (1975).
12. J. W. Boretos, W. S. Pierce, R. E. Bair, A. F. Lory, and H. J. Donachy, *J. Biomed. Mater. Res.*, **9**, 327 (1975).
13. A. Takahara, J. Tashita, T. Kajiyama, and M. Takayanagi, *Rep. Prog. Polym. Phys. Jpn.*, **24**, 737 (1981).
14. J. Tashita, A. Takahara, T. Kajiyama, and M. Takayanagi, *Rep. Prog. Polym. Phys. Jpn.*, **25**, 845 (1982).
15. A. Takahara, J. Tashita, T. Kajiyama, and M. Takayanagi, *Kobunshi Ronbunshu*, **39**, 203 (1982).
16. Y. J. P. Chang and G. L. Wilkes, *J. Polym. Sci., Polym. Phys. Ed.*, **13**, 455 (1975).
17. G. L. Wilkes and S. Abouzahr, *Macromolecules*, **14**, 458 (1981).
18. C. B. Wang and S. L. Cooper, *Macromolecules*, **16**, 775 (1983).
19. R. W. Paynter, B. D. Ratner, and H. R. Thomas, *Polym. Prepr., Am. Chem. Soc., Div. Polym. Chem.*, **24**, 13 (1983).
20. N. Ogata, K. Sanui, H. Tanaka, Y. Takahashi, E. Kitamura, Y. Sakurai, T. Okano, K. Kataoka, and T. Akaike, *J. Appl. Polym. Sci.*, **26**, 4207 (1981).
21. N. Yui, Y. Takahashi, K. Sanui, N. Ogata, K. Kataoka, T. Okano, and Y. Sakurai, *Jpn. J. Artif. Organs*, **10**, 1070 (1981).
22. N. Yui, K. Sanui, N. Ogata, K. Kataoka, T. Okano, and Y. Sakurai, *Jpn. J. Artif. Organs*, **11**, 1175 (1982).
23. N. Yui, K. Sanui, N. Ogata, K. Kataoka, T. Okano, and Y. Sakurai, *J. Biomed. Mater. Res.*, **17**, 383 (1983).
24. N. Yui, J. Tanaka, K. Sanui, and N. Ogata, *Makro-*

mol. Chem., in contribution.
25. K. Kataoka, T. Akaike, Y. Sakurai, and T. Tsuruta, *Makromol. Chem.*, **179**, 1121 (1978).
26. G. Brecher and E. P. Cronkite, *J. Appl. Physiol.*, **3**, 365 (1950).
27. A. Takahara, J. Tashita, T. Kajiyama, and M. Takayanagi, *Rep. Prog. Polym. Phys. Jpn.*, **25**, 841 (1982).
28. A. E. Woodward, J. M. Crissman, and J. A. Sauer, *J. Polym. Sci.*, **44**, 23 (1960).
29. J. L. Brash, *Ann. N. Y. Acad. Sci.*, **283**, 356 (1977).